THE NEARFIELD SPHERICAL MICROPHONE ARRAY

Etan Fisher[1] *and Boaz Rafaely*[2]

Department of Electrical and Computer Engineering
Ben-Gurion University of the Negev, Beer-Sheva 84105, Israel.
[1]fisher@ee.bgu.ac.il, [2]br@ee.bgu.ac.il

ABSTRACT

A nearfield spherical microphone array is presented. The nearfield criterion of the spherical array is defined in terms of array order, frequency and location. It is shown that given a source in the nearfield, significant attenuation of farfield interference is achieved. Also, nearfield sources may be attenuated relative to farfield sources. Dereverberation of a nearfield source in a reverberant enclosure is demonstrated using the nearfield microphone array.

Index Terms – Microphone array, Spherical harmonics, Beamforming, Dereverberation.

1. INTRODUCTION

In most microphone array processing applications, the wavefront is assumed planar. The plane wave assumption greatly simplifies the processing algorithms, but is adequate only when the source distance is much greater than the maximal array dimension [1]. In nearfield applications, the plane wave assumption may not hold, since phase and gain errors appear in the array beampattern. One possible solution is to estimate the phase and gain required for nearfield corrections, and design the array beampattern accordingly [2]. The spherical microphone array is an attractive option for the analysis of spherical wave sound fields in three dimensions, as it directly facilitates 3-D beamforming with rotational symmetry. The spherical microphone array has been previously studied for farfield spatial beamforming [3][4], and sound field measurement and analysis [5]. Some of the advantages of the spherical microphone array in the nearfield have been implemented in [6]. However, a thorough performance analysis of the nearfield spherical array has not yet been published.

In the current study, formulation for a nearfield spherical microphone array is developed, based on the radial filter suggested in [6]. After defining the nearfield criterion, the nearfield spherical microphone array is analyzed. Given a nearfield source, significant attenuation of farfield interference is achieved. Furthermore, a radial beampattern may be designed for attenuating nearfield sources relative to the farfield. Dereverberation of the response due to a nearfield source in a reverberant enclosure is presented and compared to dereverberation by a farfield array.

This research was supported by the Israel Science Foundation (ISF grant No. 155/06).

2. NEARFIELD CRITERION

Consider a unit amplitude point source located at $\mathbf{r}_s$, where $\mathbf{r}_s = (r_s, \theta_s, \phi_s)$, and r_s, θ_s and ϕ_s are the respective distance, elevation and azimuth of the spherical coordinate system [7]. Using the spherical harmonics expansion, and suppressing the harmonic time dependence throughout, the incident field at $\mathbf{r} = (r, \theta, \phi)$ assumes the form [8]

$$p(r, \Omega, k) = 4\pi ik \sum_{n=0}^{\infty} b_n(kr) h_n(kr_s) \frac{2n+1}{4\pi} P_n(\cos\Theta) \tag{1}$$

where k is the wavenumber, $P_n(\cdot)$ is the Legendre polynomial of order n, and Θ is the angle between $\Omega_s = (\theta_s, \phi_s)$ and $\Omega = (\theta, \phi)$. The farfield mode strength, $b_n(kr)$, is based on the spherical Bessel function, $j_n(kr)$, and is generalized for open or rigid arrays [3],[5]. $h_n(kr_s)$ is the spherical Hankel function of the second kind.

In [6], the normalized nearfield mode strength is defined as

$$b_n^s(kr, kr_s) = k b_n(kr) h_n(kr_s) \ . \tag{2}$$

When $kr_s \gg n$, the large argument spherical Hankel function approximation yields [7]

$$b_n^s(kr, kr_s) \approx (-i)^{n+1} b_n(kr) \frac{e^{ikr_s}}{r_s} \ . \tag{3}$$

In this case, (1) converges to a plane wave sound field [8]. Figure 1 shows the typical behavior of $b_n^s(kr, kr_s)$. At low frequencies ($kr_s \ll n$) and $b_n^s(kr, kr_s)$ becomes approximately constant. This constant value decreases with order, implying a limit on array performance above a certain order. For $kr_s \gg n$, $b_n^s(kr, kr_s)$ becomes approximately constant with n, behaving similarly to $b_n(kr_s)$ [6]. Therefore, a

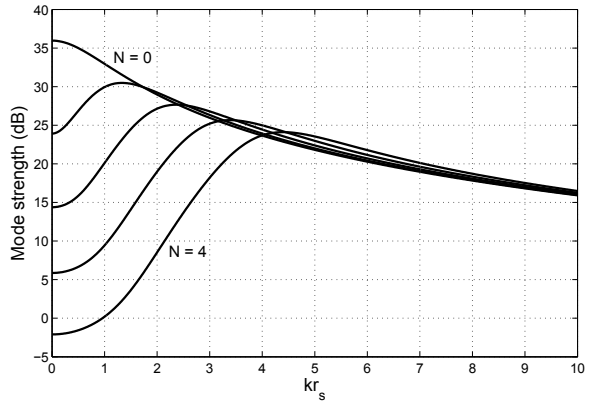

Fig. 1. The nearfield mode strength, b_n^s.

spherical microphone array of order N will exhibit nearfield behavior for $kr_s \approx n$ and lower. It may be stated that at each mode n, nearfield behavior will be evident for $kr_s < n$, and for a microphone array of order N, nearfield behavior will be evident for

$$kr_s < N \ . \tag{4}$$

The array samples the sound field at discrete locations, according to one of several pre-determined sampling schemes [9]. In this case, spatial aliasing may occur. The maximal wavenumber that can be processed without significant spatial aliasing is given by

$$k_{max} = \frac{N}{r_a} \ , \tag{5}$$

where r_a is the array radius. Substituting (5) into (4), the criterion for r_s to be in the nearfield is given by

$$r_s < r_a \frac{k_{max}}{k} = r_{NF} \ , \tag{6}$$

where r_{NF} is the nearfield extent. The significance of nearfield performance is discussed in section IV.

3. NEARFIELD SPHERICAL ARRAY PROCESSING

The spherical Fourier transform of (1) is given by [8]

$$p_{nm}(kr, kr_s, \Omega_s) = 4\pi i k b_n^s(kr, kr_s) Y_n^{m^*}(\Omega_s) \ . \tag{7}$$

In order to recover the source amplitude, [6] suggested the ideal compensation filter $1/b_n^s(kr, kr_s)$. A more general radial filter is $1/b_n^s(kr, kr_0)$, where r_0, the look distance, is chosen to yield a desired array output. The array output based on this filter is:

$$\begin{aligned} & y(kr_s, kr_0, \Theta) = \\ & = \sum_{n=0}^{N} \sum_{m=-n}^{n} d_n \frac{p_{nm}(kr, kr_s, \Omega_s)}{4\pi i b_n^s(kr, kr_0)} Y_n^m(\Omega_0) \\ & = \sum_{n=0}^{N} d_n \frac{h_n(kr_s)}{h_n(kr_0)} \frac{2n+1}{4\pi} P_n(\cos\Theta) \ . \end{aligned} \tag{8}$$

where $\Omega_0 = (\theta_0, \phi_0)$ is the look direction, Θ is the angle between Ω_s and Ω_0, and d_n are the array beampattern coefficients.

4. NEARFIELD ARRAY ANALYSIS

The behavior of the nearfield spherical array is radially dependent on the ratio between the two Hankel functions. Two parameters are defined to assist in analysis of the nearfield array performance. α is defined as the ratio between the source distance, r_s, and the look distance, r_0:

$$\alpha = \frac{r_s}{r_0} \ . \tag{9}$$

β is termed the *nearfield margin*, and is defined by

$$\beta = \frac{N}{kr_s} \ . \tag{10}$$

Following (6),when $\beta > 1$, the source will be in the nearfield. The corresponding parameter for the look distance is

$$\alpha\beta = \frac{N}{kr_0} \ . \tag{11}$$

When $\alpha\beta > 1$, the look distance will be in the nearfield. The array output of (8) is modified to

$$y(\alpha, kr_s, kr_0, \Theta) = \alpha \sum_{n=0}^{N} d_n \frac{h_n(kr_s)}{h_n(kr_0)} \frac{2n+1}{4\pi} P_n(\cos\Theta) \ , \tag{12}$$

where multiplication by α normalizes the output by the natural attenuation of point sources. This provides an examination of behavior unique to the nearfield.

4.1. Farfield source and look distances

When both r_s and r_0 are in the farfield, $\beta, \alpha\beta \ll 1$. In this case, $kr_s, kr_0 \gg n$, and (12) degenerates to the farfield array output given by [3]

$$y(\alpha, kr_0, \Theta) = e^{ik(r_s - r_0)} \sum_{n=0}^{N} d_n \frac{2n+1}{4\pi} P_n(\cos\Theta) \ . \tag{13}$$

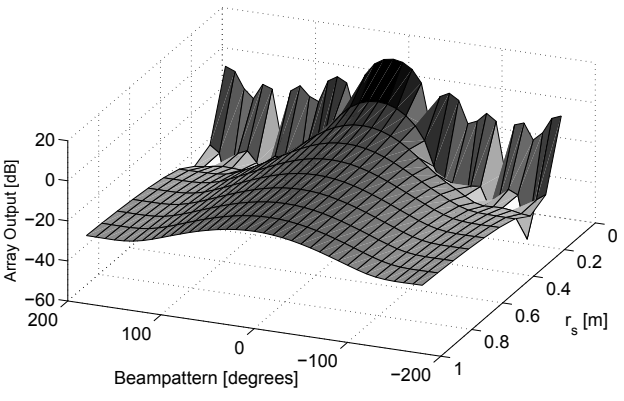

Fig. 2. Nearfield beampattern for $N = 4$, $r_a = 0.1$ meters, and $k = k_{max}/10 = 4$.

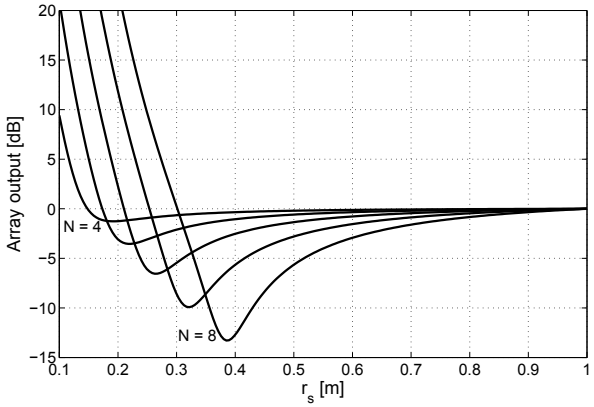

Fig. 3. Array output for $N = 4, \cdots, 8$. r_0 is in the farfield, and $k = 20$.

4.2. Nearfield source and look distances

When both distance parameters are well within the nearfield, it may be assumed that $kr_s \ll n$ and $kr_0 \ll n$. The small argument spherical Hankel function approximation yields [7]

$$y(\alpha, \Theta) = \sum_{n=0}^{N} d_n \frac{1}{\alpha^n} \frac{2n+1}{4\pi} P_n(\cos\Theta) \ . \qquad (14)$$

This array output is characterized by an exponential slope dependent solely on α. As r_s and r_0 move farther from the array, the slope decreases, converging to some farfield value.

Figure 2 shows the radially dependent beampattern of an $N = 4$ array with radius $r_a = 0.1$ meters, at $k = \frac{k_{max}}{10} = 4$. In this figure $\beta > 1$. The look distance was chosen as $r_0 = 0.2$ meters, which is in the nearfield since $\alpha\beta = 5 > 1$.

In the nearfield, a source located at $r_s > r_0$ would be attenuated relative to a source located at r_0, and a source located at $r_s < r_0$ would be amplified relative to a source located at r_0. The coefficients, d_n, were chosen to yield an optimal Dolph-Chebyshev beampattern in the farfield [10]. This beampattern is reached for $r_s = r_0$. As r_s increases, the beampattern flattens out. Below r_0, the desired beampattern is not achieved. The coefficients may be corrected using the algorithm proposed in [2].

4.3. Farfield Source with nearfield look distance

The next case is when r_0 in the nearfield and r_s is in the farfield. A farfield source would be attenuated relative to a source in the nearfield, as is evident from figure 2. When r_s is far enough from the array, the array output depends on r_0 only. In this case it may be assumed that $\alpha \gg 1$ and $\beta \ll 1$, or $kr_s \gg n$. Assuming the look distance is well within the nearfield, the Hankel function approximations yield

$$y(\alpha, kr_0, \Theta) = \qquad (15)$$
$$e^{i\alpha kr_0} \sum_{n=0}^{N} d_n (-i)^n \frac{(kr_0)^n}{(2n-1)!!} \frac{2n+1}{4\pi} P_n(\cos\Theta) \ .$$

A lower performance limit for the performance of this output may be reached. As $kr_0 \to 0$, the contribution of higher orders to the array output becomes negligible. At the limit, only $n = 0$ is significant to the array output. In this case, the magnitude of the array output for $d_0 = 1$ is

$$|y(\alpha, kr_0, \Theta)| = \frac{1}{4\pi} \ , \qquad (16)$$

which yields a constant attenuation of -22 dB.

4.4. Nearfield source with farfield look distance

When r_s is in the nearfield and r_0 is in the farfield, $\beta > 1$ and $\alpha < 1$. Assuming $kr_s \ll n$ and $kr_0 \gg n$, the Hankel approximations yield:

$$y(\alpha, kr_0, \Theta) = e^{-ikr_0} \frac{1}{4\pi} \sum_{n=0}^{N} d_n i^n \frac{(2n+1)!!}{(kr_s)^n} P_n(\cos\Theta) \ . \qquad (17)$$

The $1/(kr_s)^n$ term causes the output to diverge as $kr_s \to 0$. However, as long as the source distance can be limited to a minimum distance from the array, $r_s > r_{min}$, nearfield sources may be attenuated relative to farfield sources. Figure 3 shows the radial behavior in the look direction for arrays of order $N = 4, \cdots, 8$ calculated from (17) with $d_n = 1$. Array outputs show a clear dip at r_s values which vary with array order. Therefore, some control over the spatial location of the dip is expected to be achieved by modifying d_n, although this might change the beampattern. The

dip in the beampattern can be used for attenuating sources near the dip location relative to other farfield and nearfield sources.

5. DEREVERBERATION GIVEN SOURCES IN THE NEARFIELD

In order to demonstrate nearfield array capabilities in a multiple source environment, a reverberant enclosure ($8 \times 6 \times 4$ meters) was simulated using the image method [11]. Array parameters were chosen to be $N = 4$, $r_a = 0.1$ meters, $r_0 = r_s = 0.2$ meters, and $d_n = 1$ in order to provide unit response at the source location. The sampling scheme was arbitrarily chosen to be equiangle, requiring $4(N+1)^2$ microphones [9]. Given the source location, the directional response of (8) may be calculated directly using the inverse Fourier transform, yielding the directional impulse response (DIR). Figure 4 shows the first 30 milliseconds of the room impulse response (IR) and the directional impulse responses of the nearfield and farfield arrays. The room reverberation time (RT), calculated directly from the decay curve at -60 dB [12], was 137 milliseconds. The farfield array RT was 95 milliseconds, and the near-field array RT was 23 milliseconds, proving the dereverberation capabilities of the nearfield array. Although reverberation is not significant in the nearfield, this simulation demonstrates noise source attenuation capabilities of the nearfield array.

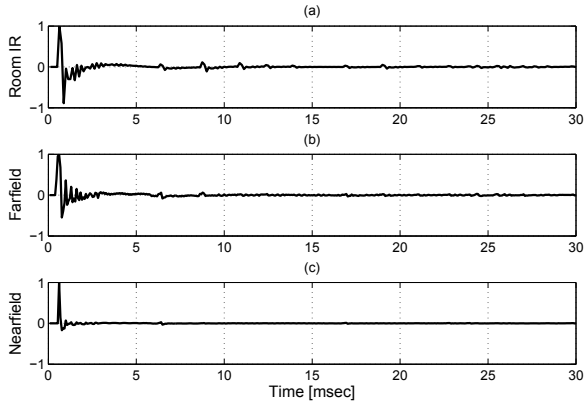

Fig. 4. (a) Room IR ; (b) Farfield array DIR ; (c) Nearfield array DIR.

6. CONCLUSION

This paper presented an analysis of the nearfield spherical microphone array. Performance analysis suggests an array with radial, as well as directional, design capabilities. It was shown that dereverberation using the nearfield array provides improved attenuation of reflections compared to the farfield array.

7. REFERENCES

[1] J.G. Ryan, and R.A. Goubran, "Array optimization applied in the near field of a microphone array," *IEEE Trans. on Speech and Audio Processing*, vol. 8, no. 2, pp. 173-176, 2000.

[2] R.A. Kennedy, T.D. Abhayapala, and D.B. Ward, "Broadband nearfield beamforming using a radial beampattern transformation," *IEEE Trans. on Signal Processing*, vol. 46, no. 8, pp. 2147-2155, 1998.

[3] J. Meyer and G.W. Elko, "Spherical microphone arrays for 3D sound recording," in: Y. A. Huang, J. Benesty (Eds.), Audio Signal Processing for Next-Generation Multimedia Communication Systems, Kluwer Academic Publishers, 2004 (Chap. 3).

[4] Zhiyun Li, Ramani Duraiswami, "Robust and Flexible Design of Spherical Microphone Arrays for Beamforming", IEEE Transactions on Speech and Audio Processing. vol. 15, no. 2, pp. 702 - 714, 2007.

[5] B. Rafaely, "Plane-wave decomposition of the sound field on a sphere by spherical convolution," *J. Acoust. Soc. Am.*, vol. 116, no. 4, pp. 2149-2157, 2004.

[6] J. Meyer and G.W. Elko, "Position independent close-talk microphone," *Signal Processing*, 86, pp. 1254-1259, 2005.

[7] G. Arfken and H. J. Weber, *Mathematical methods for physicists*. San Diego: Academic Press, 2001.

[8] E.G. Williams (1999), *Fourier acoustics: sound radiation and nearfield acoustical holography*, New York, Academic.

[9] B. Rafaely, "Analysis and design of spherical microphone arrays," *IEEE Trans. on Speech and Audio Processing*, vol. 13, no. 1, pp. 135-143, 2005.

[10] B. Rafaely, A. Koretz, R. Winik, and M. Agmon, "Spherical microphone array beampattern design for improved room acoustics analysis," International Symposium on Room Acoustics, paper no. S42, 2007.

[11] J.B. Allen, and D.A. Berkley, "Image method for efficiently simulating small room acoustics," *J. Acoust. Soc. Am.*, vol. 65, no. 4, pp. 943-950, 1978.

[12] M. R. Schroeder, "New Method of Measuring Reverberation Time," *J. Acoust. Soc. Am.*, vol. 37, pp. 409-412, 1965.